INTERNATIONAL JOURNAL OF AUTOMOTIVE AND MECHANICAL ENGINEERING (IJAME)
ISSN: 2229-8649 e-ISSN: 2180-1606
VOL. 19, ISSUE 4, 10084 – 10093
DOI: https://doi.org/10.15282/ijame.19.4.2022.05.0779

ORIGINAL ARTICLE

Throttling Effect on the Performance and Emissions of a Multi-Cylinder Gasoline Fuelled Spark Ignition Engine

Khalaf I. Hamada[1,*], M. F. Rahim[2] , M. M. Rahman[2] and Rosli A. Bakar[2]

[1]Mechanical Engineering Department, College of Engineering, Tikrit University, 34100 Iraq
[2]Faculty of Mechanical and Automotive Engineering Technology, Universiti Malaysia Pahang, 26600 Pahang Malaysia

ABSTRACT – The throttle mechanism, a regulatory technique of engine output, is accompanied by a loss of some energy. The effect of intake air throttling on the performance and emissions of a multi-cylinder spark ignition gasoline engine was experimentally investigated. The engine was coupled to a hydraulic dynamometer equipped with a customized cooling system for both the engine and dynamometer. Experimental tests were performed for various engine speeds and air-fuel ratios at the WOT and POT conditions with optimized ignition timing. The acquired results recorded that a better engine operation could be achieved with WOT in terms of *bmep*, *bsfc*, η_b, CO, CO_2 and UHC compared to POT. At the same time, the worst trend at WOT was noticed for the NO_x concentration due to the higher conversion efficiency of fuel combustion. In terms of engine speed for both WOT and POT conditions, operating at 3000 rpm represents the minima of ϕ, *bsfc*, CO and UHC; and the maxima of η_b, CO_2 and NO_x with some fluctuation on both sides of this point. Maximum recorded values of η_b were about 30.55% and 28. 55%, while the minimum values of *bsfc* were about 274 and 293 g/kW.h for the WOT and POT conditions, respectively. The maximum *bmep* was obtained at 2500 rpm at WOT and POT conditions with values of about 940 kPa and 904 kPa, respectively. Maximum recorded values of NO_x were about 1525 and 977 ppm for the WOT and POT conditions, respectively.

ARTICLE HISTORY
Received: 26th Oct. 2020
Revised: 22nd Nov. 2022
Accepted: 10th Dec. 2022
Published: 28th Dec. 2022

KEYWORDS
Part load;
Throttle position;
Naturally aspirated;
Carburetted engine

INTRODUCTION

Internal combustion engine (ICE) is the leading technology employed as the power generator of various vehicles and steering the transportation sector for more than 100 years. Among different categories of ICEs, spark ignition (SI) is one of the most favourable prime movers for passenger vehicles [1],[2]. Several mechanisms have been implemented to achieve a regular and smooth operation of SI engines under various conditions. For example, a reduction technique of engine output torque is required for all spark ignition (SI) engines to meet their load and speed range [3]. To match this requirement for conventional carburetted SI engines, the airflow is usually restricted by the intake throttle plate, which governs the fuel flow through the carburettor [4], as well as controls the air quantity which enters into the combustion chamber [5]. As a result of throttle restriction, the manifold absolute pressure (MAP) falls below atmospheric pressure through the intake manifold. This prevents airflow into the cylinder as the piston descends; thereby, the induced fresh charge would be less than its amount at un-throttled conditions [6]. To compensate for this reduction, the engine should perform extra work on the piston, which increases the intake pumping losses. As a result, under part load conditions, engines use some of the work to pump air across the partially closed throttle valve [7]. Consequently, the thermal efficiency of the spark ignition engine, which is running at low loads, is reduced due to the effect of the throttle valve that controls the engine load and by the fact that the compression starts at low pressure [8]. Furthermore, the reduction of airflow into the engine cylinder causes a lack of oxygen, leading to incomplete combustion of the fuel-air mixture. Subsequently, undesirable exhaust gas emissions could be produced from the engine running under such conditions [9].

Numerous techniques have been adopted on conventional carburetted engines to mitigate pumping losses. One of the oldest approaches is adopted the concept of the Miller cycle engine to diminish this type of loss. The Miller cycle engine is characterized by its long expansion stroke compared to the conventional Otto cycle engine [10]. It was a candidate for the concept of Miller cycle to simulate engine operation under part load conditions instead of the traditional Otto cycle [11]. Furthermore, an adjustment of the compression ratio and the variation of valve timing has revealed that a substantial enhancement could be achieved [12]. Further developments were latterly introduced, including the exhaust gas recirculation (EGR), variable valve timing (VVT) and lift, variable compression ratio, stratified charge lean burn engine, and variable displacement [13],[14]. Also, turbine throttling, valve throttling, supercharger de-throttling, and cylinder deactivation were recently implemented to reduce or even eliminate the use of a conventional throttle. However, unbalanced vibration and cooling were commonly stimulated to be overcome with these technologies [15]. A significant reduction in throttle loss was achieved based on the downsized concept of naturally aspirated gasoline engines. However, a rather great throttling loss is still recorded under part load operation, even for extremely downsized engines [16]. The fuel injection strategy was introduced as an alternative technique to regulate the engine load in diesel engines. It is

*CORRESPONDING AUTHOR | Khalaf | ✉ dr_khalafih@tu.edu.iq

comparable to wide open throttle (WOT) conditions in terms of operating without restrictions imposed by the throttle valve in SI engines. Even if it reduces engine pumping losses, it is limited by operating outside fuel stoichiometry in Otto cycle engines [17].

Tremendous developments have been accomplished on ICEs which are mostly focused on improving engine performance and reducing harmful emissions. Abdullah and his co-authors [9] studied the influence of pressure drop caused by air filters across the intake manifold on the performance and emission of small gasoline SI engines. It was revealed that a higher pressure of intake air could be acquired by eliminating air filters, which reduces the airflow restriction in the air intake system. Accordingly, a better combustion process was achieved due to higher air availability, which improves power output and fuel economy and reduces exhaust emissions. Rashid and his co-authors [4] studied the influence of the octane value of gasoline fuel on the performance and emission of SI engines. Three octane values of gasoline fuel were tested, namely, RON95, RON97 and RON102. Experiments were performed at various engine speeds, ranging from 1000 to 3500 rpm in steps of 500 rpm, with a constant throttle position of 18%. It was revealed that the higher engine brake torque, power and thermal efficiency were achieved with a higher RON while using the RON97 reduced the brake-specific fuel consumption by about 5–10% compared to RON102 and RON95. Regarding engine emissions, the lowest concentration of NO_x was recorded with the RON102 fuel; however, it was conjugated with the production of the highest concentration of CO and HC. Finally, it was recommended to use the RON97 fuel, for Malaysian engine models with the newest technology, due to its' higher performance and efficiency as well as the most environmentally friendly. Jahirul and his co-authors [18] experimentally compared the performance and emissions of gasoline and CNG fuel injection SI engine. Tests were performed with various engine loading ranging from 25% to 65% of full load over a wide range of engine speeds at 50 and 80 % throttle positions. It was concluded that the 50 % throttle position worsens CNG and gasoline-fuelled engines' performance parameters and CO emission. However, the engine test at full throttle position was avoided for safety as the continuous operation on the CNG produced high exhaust gas temperature. Aljamali and his co-authors [19] experimentally compared the performance and emissions of gasoline and CNG-fuelled port injection SI engine. Tests were performed with a full load over a wide range of engine speed 1000 to 6000 rpm, at 50 and 100 % throttle positions. It was revealed that there is no big difference between the results at 50 and 100 % throttle positions for gasoline and CNG fuelled engines. Based on Kilicarslan and Qatu [20], there are not many studies concerning the emission characteristics of gasoline engines in terms of engine speed. So, they conducted an experimental analysis of the exhaust gas emission of a gasoline-fueled engine to introduce contribution research in this area. The engine tests were performed based on various speeds at 60 % throttle position. It was concluded that a similar trend of NO_x and CO emissions with engine speed while the SO_2 behave differently.

Sun and his co-authors [21] compared the throttled and unthrottled SI engines in terms of the pumping losses at low-to-medium loads. An early intake valve closing was fully controlled based on a variable valve hydraulic system instead of the traditional throttle valve. The unthrottled SI engine was improved by reducing the pumping losses by about 81% at 2000 rpm and the bsfc by about 4.1% to 11.2% at 2000 and 3000 rpm, respectively. Kardan and his co-authors [22] investigate the influences of varying throttle positions on the performance and emissions of a nonconventional (crank-rocker) engine. Experiments were performed with various throttle positions (25%, 50%, 75% and 100%) at constant engine speed and ignition timing of 2000 rpm and 6.5o bTDC. It was revealed that a throttle position of 75% acquired the best engine performance in terms of brake torque, power, bsfc and thermal efficiency. Moreover, the emissions trends behaved comparably to the conventional (crank-slider) engines until the throttle position of 75%. The throttle opening of the crank-rocker engine wider than 75% leads to the emissions oppositely behaved due to choking of the intake charge. Accordingly, it was recommended that larger inlet ports should be adopted to improve the performance of such engine types. A comparison of the gasoline and methane fuelled SI engines based on the environmental characteristics was performed by Dimitrov and his co-authors [23]. The experiments were performed under WOT and various engine speeds with the optimum setting of the spark timing and the air-to-fuel mixing for both tested fuels. It was revealed that the methane-fuelled engine ensures a homogeneous air-fuel mixture over the entire engine speed range, which is not achieved by a gasoline-fuelled engine. Accordingly, the lower levels of harmful exhaust emissions were attended to due to an improved combustion process. The influence of the engine load based on partial throttle openings (25% and 75% of WOT) in low and high conditions was investigated by Yontar and Doğu [24] for gasoline and CNG fuelled SI engines. It was concluded that engine brake torque and power, as well as the exhaust emission, were dropped while the bsfc was increased as the throttle opening lowered due to less air induced.

It is generally true that research investigations dealing with the performance of internal combustion engines are carried out at full load conditions. However, for the greater portion of their lifetime, motor-car engines operate at part-load [24-25], therefore, investigating the engine efficiency at part-load is of great importance. Conventional gasoline engines use a throttle to control the engine load, causing substantial pumping losses at part load [26]. Moreover, the engine speed is mainly governed by the pressure drop across the intake manifold of a naturally aspirated engine [27]. It is expected that the SI engine has a poor part-load performance compared to the full-load conditions. Besides that, the performance of ICE and its pollutants are strongly correlated together. So, the impact of load conditions on the performance and emissions for such types of engines should reveal concurrently [28]. Based on the summarized literature survey above, the influence of throttle position and engine speed was conducted mostly for fuel injection engines other than carburetted type. Hence, the purpose of this manuscript is dedicated to investigating the effect of engine speed on the performance and emission of carburetted type SI engine under wide-open throttle (WOT) and part-open throttle (POT) conditions. An experimental setup, as well as test procedures, was implemented for a certain multi-cylinder naturally-aspirated gasoline automobile

engine. Through a robust experimental setup and procedure, a diagnostic analysis can be achieved for the performance and emissions of the tested engine under part and full-throttle opening conditions.

EXPERIMENTAL APPARATUS

This section is devoted to reporting the main components of the experimental setup and measurement techniques. The experimental setup consists of a detailed description of the experimental engine test rig and important parameters. The engine test rig was developed using in-lab facilities and tested for a wide range of speeds and loads. A schematic of the experimental setup with all details of the main components and connections is presented in Figure 1. This test rig was basically proposed to validate the predictability of a one-dimensional engine model of simulating the processes in a gasoline fuelled (RON97) SI engine [29]. Measurement data include the engine torque, engine speed, cylinder pressure, rate of air and fuel consumption, ignition timing and engine emissions. The experimental setup of the tested engine is built based on the ATE-60 hydraulic dynamometer, which has a maximum capacity of 170 hp at 7000 rpm. The hydraulic dynamometer is coupled to the baseline research engine, which is a multi-cylinder, in-line arrangement, gasoline (Otto) engine. Its original intake system is naturally aspirated, and the mixture formation system is carburetted in design. Table 1 lists the details of the engine specifications. The engine specification remains unchanged except for the cooling system, which has been modified to incorporate external and portable characteristics. The coolant temperature is controlled physically based on the instantaneous cooling water outlet temperature. To fulfil an optimum operation, a sufficient supply of water is fed to the dynamometer and the engine. The dynamometer water supply is pressurized in the range of 1.0-1.75 bar for operations ranging from 1000 to 5000 rpm. To supply the water as well as to release the heat generated by the dynamometer operation, a customized cooling system that consists of a heat exchanger, cooling fan and special water reservoir is connected with the outlet water pipeline.

As for the engine, a sufficient flow rate of water is required to cool down the engine, especially when running at full power. The mass flow rate of water in the range of 4 to 15 litres per minute is supplied accordingly, appropriate to engine speed and load. The engine torque was evaluated using an S-type load cell coupled to the dynamometer's arm. The maximum deviation of the load cell was about 2.3% based on in-lab calibration. The engine speed was specified by means of the crank angle encoder of Kistler (Type 2613B). The crank angle encoder transmits the signal to the combustion analyzer for recording and display. The cylinder pressure is indicated based on the measurement of the combustion pressure sensor of Kistler TM (Type 6117), which is a spark plug-type pressure transducer. Cylinder number one was set as the reference for the combustion pressure measurement. The fuel flow rate was gauged manually based on the gravimetric method. The elapsed time interval for consumption of a specified volume (50 ml) of fuel in a bulb glass tube was pointed out. A predictable method of differential-pressure measurement was adopted for monitoring the air flow rate based on an orifice plate meter.

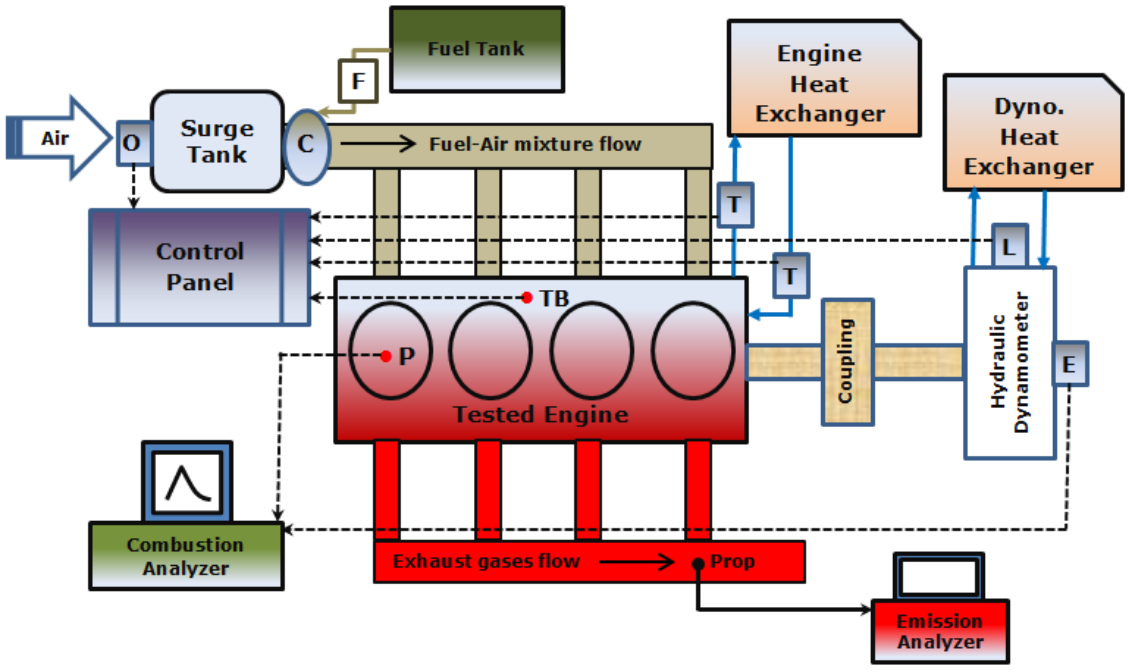

C	Carburettor	**E**	Crank angle encoder	**F**	Fuel flow meter
L	Load cell	**P**	Pressure transducer	**O**	Orifice plate meter
T	Temperature sensor	**TB**	Throttle body	----	Signal line

Figure 1. Schematic of the experimental setup

The airflow meter is located upstream of a surge tank which is used to dampen the flow pulsation in the intake system. The maximum deviation of the airflow meter was about 3.5% at the tested flow conditions (1500 rpm to 6000 rpm). A

stroboscope-based measurement kit labelled Strobo-tester (Model DG83-D) product was employed for ignition timing measurement. An in-lab fabricated mechanism was tailored and tuned with the throttle body to control the carburettor opening. The fabricated mechanism is composed of a cable and a threaded bolt moving inside a nut fixed on the instrumentation panel. Accordingly, engine testing can be performed under part and wide-open throttle conditions. The exhaust gas composition of the engine was analyzed by the gas analyzer kit. The model of KEG500 of KOEN gas analyzer was utilized to measure the species concentration of the exhaust gas. It is utilized to measure of CO_2 (0.0–20.0%), CO (0.00–9.99%), HC (0–9999 ppm), and NO_x (0–5000 ppm). Furthermore, it also measures the air-fuel ratio (0.0 – 99.0) and air surplus rate (lambda-λ) (0–2.000).

Table 1. Specifications of test engine

Parameter	Size and feature		
Engine type and model	4-stroke, spark-ignition, 4-cylinder,Mitsubishi Magma		
Bore x Stroke (mm×mm)	75.5 ×82.0		
Displacement (cm^3)	1488		
Compression ratio	9.2:1		
Max. (or nominal) Power	66 kW@6000 rpm		
Max. (or nominal) Torque	124 Nm@3000 rpm		
Valve train type	In-line OHV, SOHC, 3 valves per cylinder (two intake valves and one exhaust valve)		
Valve events (°CA)	Intake	Open	15° bTDC
		Close	63° aBDC
	Exhaust	Open	57° bBDC
		Close	13° aTDC

TEST PROCEDURE AND DATA REDUCTION

The test engine was loaded through a hydraulic dynamometer, which controls the applied load on the engine by adjusting the water flow rate. The test procedure is based on the 'position-speed mode' test sequence. In this mode, the throttle position continues to be set for a specified condition, but the dynamometer is equipped with an automatic controller, which adjusts the torque absorbed by the machine to maintain the engine speed constant, whatever the throttle position and power output. This is a very stable mode, and it is generally used for plotting engine torque–speed curves at full and part throttle openings [30]. The throttle opening and engine speed are considered independent variables. Currently, the throttle opening is controlled to achieve 50% and 100% opening, while the engine speed is set independently to satisfy the selected engine speed condition. The dynamometer load is then imposed to achieve the highest possible engine torque in that condition [31]. Hence, other variables, such as engine torque, power, and emissions are considered dependent variables. The data collection is carried out from 1500 rpm to 4000 rpm with an interval of 500 rpm based on engine speed. The engine test was repeated three times, and an average arithmetical value for each parameter was considered. To warm up the engine for operating temperature, it is started on a very rich fuel-air mixture ratio. After the engine has been run for about 5 minutes on the rich setting, the mixture is leaned somewhat and the engine is again allowed to run for the same duration.

After the warming-up period, the engine was tested at a specified speed of 1500 rpm. Then, increase the throttle opening until the engine overshoot up to 1500-2000 rpm. At that instantaneous engine speed, the brake load increased until the speed reduced to 1500 rpm, and allowed the engine to stabilize before applying any load or throttle opening. As the engine stabilized, the throttle opening increased until the engine overshoot up to 1500-2000 rpm again. Then, the brake load increased to reduce the engine speed down to the stabilized engine speed of 1500 rpm. This sequence is continued until the throttle opening achieves the specified throttle opening (50% or 100% opening) at that specified engine speed (here, 1500 rpm). As the specified throttle opening is achieved, there is no need to apply any more loads on the engine. After the engine come to stabilize the condition, recording the required data is started. Thus, the brake load is a dependent variable, whereas the engine speed is an independent variable, and the throttle opening is the controlled variable. Following this, the throttle opening is reduced and unloads the engine gradually until the engine return to the idle state. The above procedure was considered for an engine speed of 2000 rpm, 2500 rpm, 3000 rpm, 3500 rpm and 4000 rpm. The measurement of the AFR was based on the exhaust gas analyzer because it is more precise [32].

In order to evaluate the trustworthiness of the measured results, the results must be compared in terms of more general and convenient parameters. These are enabled by deriving values for brake mean effective pressure (*bmep*), brake specific fuel consumption (*bsfc*) and brake thermal efficiency (η_b). The engine output torque and power at the crankshaft, when related to the engine displacement, are generating another performance parameter called the brake mean effective pressure (*bmep*). It is a measure of work output from an engine and not of the pressures in the engine cylinder. Brake mean effective pressure is used to compare the performance of differing engine capacities and the number of cylinders. It is measured in kPa, and can be expressed as [6]:

$$bmep = \frac{P_b \times n_r \times 60}{2\pi \times N \times V_d} \quad (1)$$

where n_r the number of crank revolutions for one complete cycle, which is 2 for a four-stroke engine, N engine speed in rpm, and V_d the total volume of the engine cylinders in m^3. The brake power, P_b, delivered by the engine and absorbed by the dynamometer is the product of torque and angular speed [6].

$$P_b = \frac{2\pi \times N \times \tau}{60000} \tag{2}$$

where τ is the brake torque applied to the cradled housing in N.m. It was measured based on an attached load cell to the dynamometer's arm. The load cell was calibrated by applying a specified load amount and comparing the acquired record of the load cell to the theoretical value. Based on this in-lab calibration, the maximum deviation of load cell was about 2.33%. The specific fuel consumption based on the brake power (*bsfc*) was evaluated according to the following expression [6]:

$$bsfc = \frac{\dot{m}_f \times 3600}{P_b} \tag{3}$$

where $\dot{m}_f$ is the consumed mass of fuel during a test period. Engine thermal efficiency based on the brake power (η_b) is estimated by adapting the following expression [6]:

$$\eta_b = \frac{P_b}{\dot{m}_f \times LCV \times \eta_c} \tag{4}$$

where $\dot{m}_f$ is the consumed mass of fuel during a test period in kg/s, *LCV* is the lower calorific value of the fuel (kJ/kg), and η_c is the combustion efficiency.

RESULTS AND DISCUSSION

This section divides the acquired results from the experimental test rig into two distinctive parts, which are engine performance results and exhaust pollutants results. Engine performance and exhaust pollutants results consist of the measured data and the subsequently evaluated parameters. Measurements were carried out for the engine over a speed range from 1500 to 4000 rpm with a step change of 500, which represent the road load conditions for automobiles engine.

Engine Performance

The performance of the engine in terms of brake mean effective pressure (*bmep*), brake specific fuel consumption (*bsfc*) and brake thermal efficiency (η_b) were investigated for a wide range of engine speeds under *WOT* and *POT* conditions. The main parameter that governs engine performance and emission is the equivalence ratio (ϕ); therefore, its trends under tested conditions will be presented first. The variation of the measured ϕ as a function of engine speed at *WOT* and *POT* conditions is presented in Figure 2(a). Based on the graph, the ϕ is completely located in the rich mixture region. The stoichiometric mixture ratio for ICEs operation corresponds to the ϕ value of 1. Greater than this limit indicates a richer mixture achieved and vice versa. According to Figure 2(a), there is a fluctuation in the trend of equivalence ratio with engine speed for both *WOT* and *POT* conditions. Although, there is a minimum (or leanest) point produced at an engine speed of 3000 rpm with ϕ values of about 1.04 and 1.13 at *WOT* and *POT*, respectively. The coincidence of this minimum point for both throttle conditions concludes that the engine reached its peak breathing capacity. On the other hand, a richer mixture is achieved on both sides of this point because of the deteriorating engine breathing capacity. Generally, the trend of ϕ under *POT* is always higher than that one under *WOT* due to the lack of induced air as a result of flow restriction and less air enters the throttle body at *POT* [6]. Generally, the trend of ϕ with decreasing throttle opening is matched with the finding of Jahirul and his co-authors [18].

Figure 2(b) reveals trends of the *bmep* versus engine speed at *WOT* and *POT* conditions. There was a tendency for the *WOT* condition to produce a higher value of *bmep* over the entire range of engine speed. This basically is due to an increase in the friction mean effective pressure, as a result of increasing vacuum in the intake manifold, where the pumping losses grow as the throttle opening reduces. Furthermore, a fluctuating trend of the *bmep* with engine speed was detected only in the case of *WOT* condition. Although, it is worth noting that the maximum point of *bmep* was coincidental at 2500 rpm for both *WOT* and *POT* conditions. The maximum values were about 940 kPa and 904 kPa at *WOT* and *POT* conditions, respectively. The evaluated *bmep* gives values in the range of 870 kPa and 940 kPa at *WOT*; and in the range of 841 kPa and 904 kPa at *POT*. The naturally aspirated, medium size SI gasoline engines are characterized by the typical range of 850 to 1050 kPa of the *bmep* [6]. Accordingly, it can be concluded that the achieved results are in the acceptable range for SI engines. Even though the trend of the *bmep* with throttle opening disagreed with the findings of Aljamali and his co-authors [19], their result (in terms of the *bmep*) is doubtful due to its inconsistency with the recorded trends of the brake power.

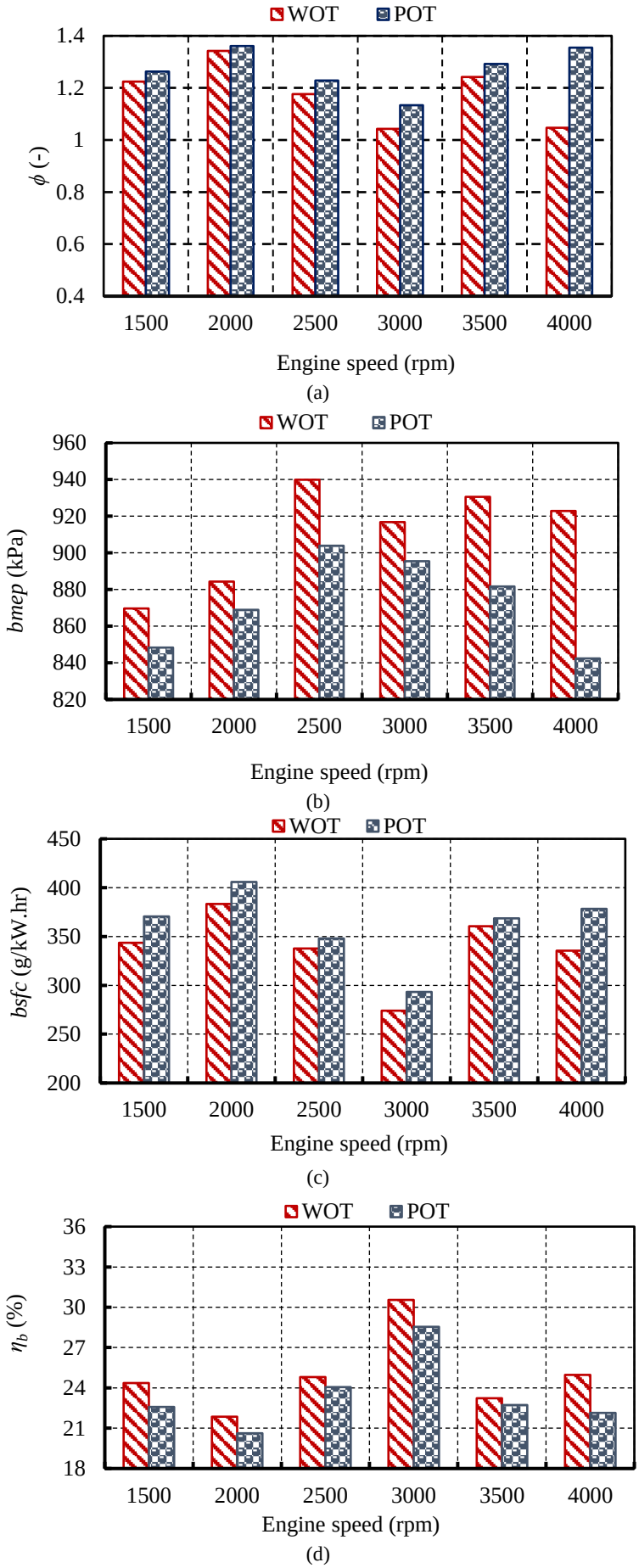

Figure 2. Variation of (a) equivalence ratio and (b) brake mean effective pressure, (c) brake specific fuel consumption, and (d) brake thermal efficiency, versus engine speed

Figure 2(c) shows the variations of *bsfc* versus engine speed at *WOT* and *POT* conditions. Generally, the *bsfc* is higher for the *POT* condition for all tested points. This general trend of the *bsfc* with decreasing throttle opening coincides with previously published works [18-19]. Such a trend is expected as the deficiency of airflow at *POT* condition (see Figure 2(a) above), and consequently, a richer mixture is delivered to the engine. It can be seen that the minimum values of the *bsfc* were located at 3000 rpm under the *WOT* and *POT* conditions. It was recorded that the minimum values of *bsfc* were about 274 and 293 g/kW.h for the *WOT* and *POT* conditions, respectively. Moreover, it is worth noting that there is a coincidence between the lowest *bsfc* and leanest points of the mixture, see Figure 2(a) above. This interrelationship between the *bsfc* and ϕ is highlighted in detail by Stone [6], where the air discharge increases with a pressure drop across the intake manifold. This brings a lower ϕ and reduces *bsfc* of the engine. Moreover, this trend is identically followed by the previously reported work by [33] at full load (*WOT*) condition.

The trends of η_b for various engine speeds at *WOT* and *POT* conditions are presented in Figure 2(d). Again, there is a tendency for the *WOT* condition to produce a higher value of η_b over the entire range of engine speed. It can be seen that the maximum values of the η_b were located at 3000 rpm under the *WOT* and *POT* conditions. It was recorded that the maximum values of η_b about 30.55% and 28.55% for the *WOT* and *POT* conditions, respectively. Such rising in brake thermal efficiency with increasing throttle opening was also noticed by Jahirul and his co-authors [18]. Furthermore, it is worth noting that there is a coincidence between the maximum and minimum points of the η_b and *bsfc* values, see Figure 2(c). This link between the trends of the ηb and *bsfc* basically reflects their reciprocal interrelationship. Such interrelated trends of the η_b and *bsfc* were indicated by previously published work [24,34].

Exhaust Pollutants

The exhaust pollutants (emissions) of the engine, which including of CO, CO_2, unburned HC and NO_x emissions, were investigated under various engine speeds and throttle positions. Figure 3(a) shows the variation of CO concentration, on volume percentage based, versus engine speed at WOT and POT conditions. One of the most important variables affecting the emissions in the exhaust of ICE is the equivalence ratio (ϕ). The substantial production of CO emission in the SI engines is caused due to running a rich mixture. This is essentially due to the oxygen deficiency to completely combust the entire carbon in the fuel into CO_2. In terms of the throttle effect, it can be noted that there is a tendency to decrease CO concentration with the increase in the throttle opening. At the POT condition, the airflow into the engine is restricted to a limited amount which operates the engine with a more probability of incomplete combustion. This general trend of the CO concentration with decreasing throttle opening coincides with previously published work [18, 24]. Moreover, this trend is identically followed of the previously reported work by [33] at full load (or WOT) condition. On the other hand, there is a minimum point of CO fraction versus engine speed, which coincides with one of the best performance characteristics (η_b and *bsfc*) at 3000 rpm. It was recorded that the minimum values of CO were about 1.83% and 4.47% for the *WOT* and *POT* conditions, respectively. These behaviours are basically related to the induced amount of air in the combustion chamber.

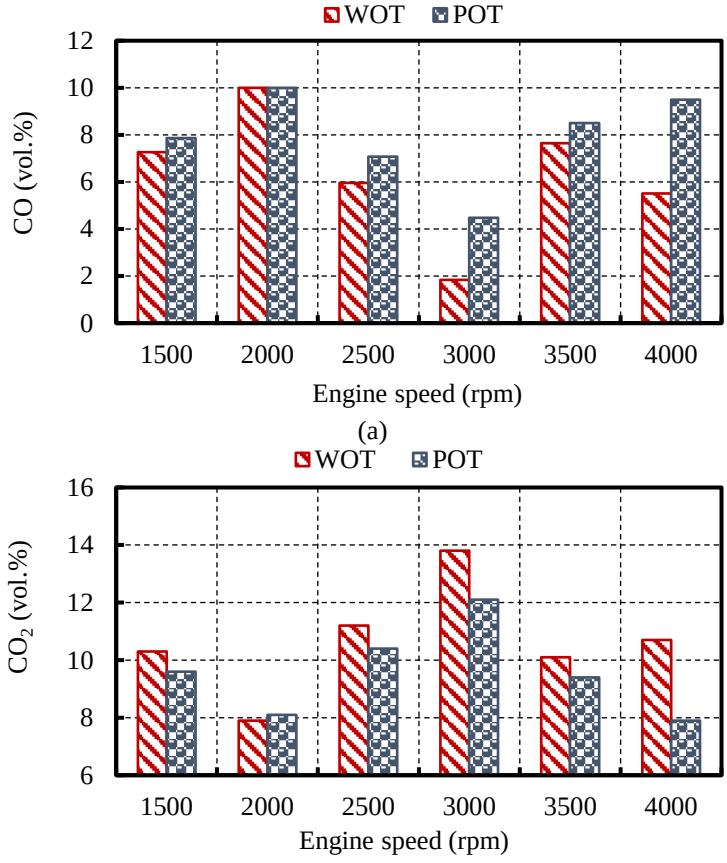

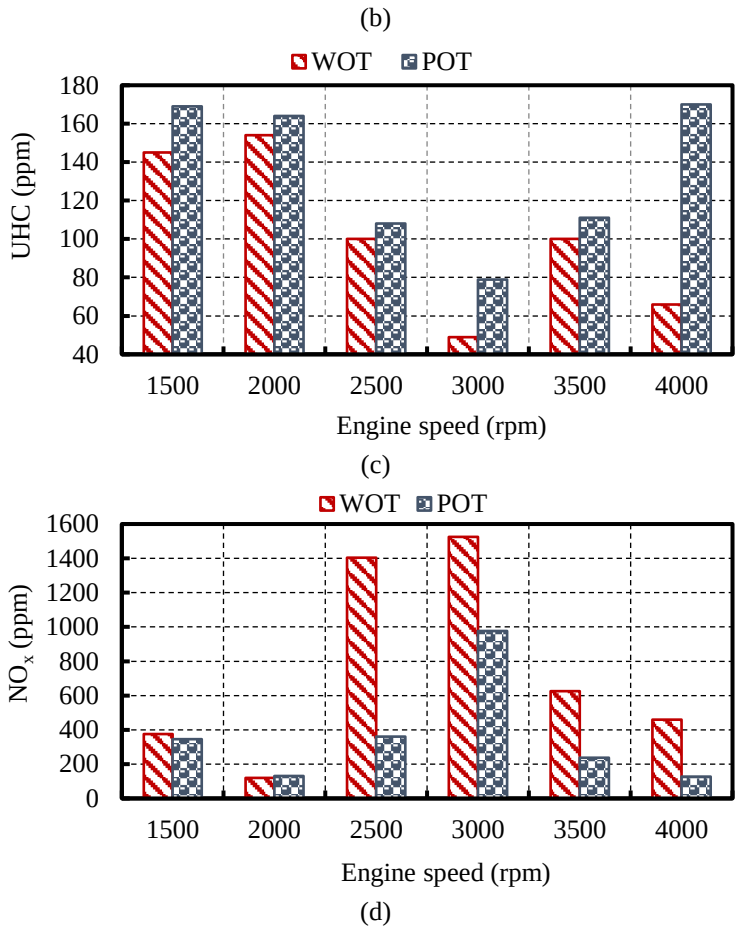

Figure 3. Variation of (a) CO, (b) CO_2 (c) UHC and (d) NO_x fractions versus engine speed

Figure 3(b) reveals the variation of CO_2 concentration, on volume percentage based, versus engine speed at POT and WOT conditions. Basically, the behaviour of CO_2 represents an inversion of the CO trends as they are interrelated to each other. It can be noted that there is a tendency to increase CO_2 concentration with an increase in the throttle opening. Such trends are due to more air induced into the combustion chamber which leads to almost complete combustion of the mixture [9]. This general trend of the CO_2 concentration with increasing of throttle opening coincides with previously published work [18, 24]. Moreover, this trend is identical to the previously reported work by [33] at full load (or WOT) conditions. On the other hand, there is a maximum point of CO_2 fraction versus engine speed, which coincides with one of the best performance characteristics (η_b and *bsfc*), at 3000 rpm. It was recorded that the maximum values of CO_2 were about 13.8% and 12.1% for the *WOT* and *POT* conditions, respectively. These behaviours are basically related to the induced amount of air in the combustion chamber. Besides that, there is some fluctuation in trends of CO_2 concentration on both sides of this point. The recorded concentrations of CO_2 were about 7.9-13.8% and 7.9-12.1% at WOT and POT conditions, respectively, over the entire engine speed range.

Figure 3(c) displays the variation of *UHC* concentration, in part per million, versus engine speed at WOT and POT conditions. Fundamentally, the UHC is frequently produced by an unburned mixture of fuel-air beside other sources including partial combustion and engine lubricant [32]. The trends of UHC concentration in Figure 3(c) are almost comparable to the CO emission trends in Figure 3(a), as both of them are commonly affected by the equivalence ratio (ϕ). In terms of the throttle effect, it can be noted that there is a tendency to decrease UHC concentration with an increase in the throttle opening. At the POT condition, the airflow into the engine is restricted to a limited amount which operates the engine with a more probability of incomplete combustion. This general trend of the UHC concentration with increasing throttle opening coincides with previously published work [18, 24]. Moreover, this trend is identically followed of the previously reported work by [33] at full load (or WOT) condition. On the other hand, there is a minimum point of UHC concentration versus engine speed, which coincides with one of the best performance characteristics (η_b and *bsfc*), at 3000 rpm. It was recorded that the minimum values of *UHC* were about 50 and 80 ppm for the WOT and POT conditions, respectively. These behaviours are basically related to the induced amount of air in the combustion chamber. Besides that, there is some fluctuation in the trend of UHC concentration at WOT conditions beyond this point. The recorded concentrations of UHC were about 50–155 ppm and 80-170 ppm at WOT and POT conditions, respectively, over the entire engine speed range.

Figure 3(d) demonstrates the variation of NO_x concentration, in part per million, versus engine speed at WOT and POT conditions. The production of NO_x is directly related to the behaviour of the combustion process and is typically governed by the maximum combustion temperature, which is known as the Zeldovich mechanism [6]. It can be noted that the WOT condition produces a higher level of NO_x concentration compared to the POT condition, almost for the entire

engine speed range. These trends are appeared due to the more air induced into the combustion chamber which leads to almost complete combustion of the mixture and higher fuel conversion efficiency [9]. This general trend of the NOx concentration with increasing throttle opening coincides with previously published work [18, 24]. Moreover, this trend is identical to the previously reported work by [33] at full load (or WOT) conditions.

On the other hand, there is a maximum point of NO_x concentration versus engine speed, which coincides with one of the best performance characteristics (η_b and *bsfc*), at 3000 rpm. It was recorded that the maximum values of NO_x were about 1525 and 977 ppm for the WOT and POT conditions, respectively. These behaviours are basically related to the trends of the mixture equivalence ratio. The enhanced combustion process leads to producing a higher in-cylinder temperature in the case of WOT condition. Accordingly, these results are well agreed with the theory of the Zeldovich mechanism. Besides that, there is some fluctuation in trends of NO_x concentration before the maximum point. The recorded concentrations of NO_x were about 119 – 1525 ppm and 128-977 ppm at WOT and POT conditions, respectively, over the entire engine speed range. Finally, Figure 3 (a)-3(d) reveal that the leanest point is produced at an engine speed of 3000 rpm, as seen earlier in Figure 2, which means the closest preferred point to complete combustion (stoichiometry).

CONCLUSIONS

Current work is dedicated to revealing experimentally the influence of throttle position on the performance and emission of the naturally aspirated SI gasoline carburetted ICE. Based on the earlier presented results, the following bullets can be concluded on this issue:

i. The WOT positively affected the engine breathing capacity compared to the POT for the entire tested range of engine speed.
ii. The WOT produces higher engine performance compared to the POT for the entire tested range of engine speed.
iii. The WOT positively affects the trends of the CO, CO_2 and UHC concentrations, whereas it negatively on the trends of the NO_x concentration compare to the POT for the entire tested range of engine speed.
iv. There is a certain engine speed for the current tested engine, mostly 3000 rpm, which gives the best engine operation, which is coincident with WOT and POT conditions.

ACKNOWLEDGEMENT

The authors appreciate the given opportunity to utilize the laboratory facilities for performing the experimental work at University Malaysia Pahang.

REFERENCES

[1] L. Durao, J. Costa, T. Arantes, F.P. Brito, J. Martins, and M. Gonçalves, "Performance and emissions of a spark ignition engine operated with gasoline supplemented with pyrogasoline and ethanol," *Energies*, vol. 13, p. 4671, 2020.
[2] A. Mazumder, A. Hasan, A.H. Ayon, and D.H. Ahmed, "Energy recovery from exhaust gas of diesel and petrol engine by turbo-electric generator," *Int. J. Automot. Mech.*, vol. 19, pp. 9823 – 9833, 2022.
[3] O.M. Ali, "Utilization of chemical waste additives with low octane commercial gasoline fuel to enhance the performance of SI Engines," *Int. J. Automot. Mech.*, vol. 18, pp. 8612 – 8620, 2021.
[4] A.K. Rashid, M.R. Abu Mansor, W.A. Wan Ghopa, and Z. Harun, "An experimental study of the performance and emissions of spark ignition gasoline engine," *Int. J. Automot. Mech.*, vol. 13, pp. 3540-3554, 2016.
[5] N.S. Mustafa, N.H.A. Ngadiman, M.A. Abas, and M.Y. Noordin,"Application of Box-Behnken analysis on the optimization of air intake system for a naturally aspirated engine," *Int. J. Automot. Mech.*, vol. 17, pp. 8029–8042, 2020.
[6] R. Stone, *Introduction to internal combustion engines*. Fourth ed. Great Britain: MacMillan Publisher, 2012.
[7] M.A. Abd Halim, N.A.R. Nik Mohd, M.N. Mohd Nasir, and M.N. Dahalan, "Experimental and numerical analysis of a motorcycle air intake system aerodynamics and performance," *Int. J. Automot. Mech.*, vol. 17, pp. 7607–7617, 2020.
[8] B. Ribeiro, J. Martins, and A. Nunes, "Generation of entropy in spark ignition engines," *Int. J. Thermodyn.*, vol. 10, pp. 53 – 60, 2007.
[9] N.R. Abdullah, N.S. Shahruddin, A.M.I. Mamat, S. Kasolang, A. Zulkifli, and R. Mamat, "Effects of air intake pressure on the engine performance, fuel economy and exhaust emissions of a small gasoline engine," *J. Mech. Eng. Sci.*, vol. 6, pp. 949-958, 2014.
[10] O.K. Demirci, A. Uyumaz, S. Saridemir, and C. Cinar, "Performance and emission characteristics of a miller cycle engine," *Int. J. Automot. Eng. Technol*., vol. 7, pp. 107-116, 2018.
[11] R. Flierl, and M. Kluting, "The third generation of valve trains-new fully variable valve trains for throttle-free load control," SAE Technical Paper 2000-01-1227, 2000.
[12] J. Martins, K. Uzuneanu, and B. Ribeiro, and O. Jasansky, "Thermodynamic analysis of an over-expanded engine," SAE Technical Paper 2004-01-0617, 2004.
[13] O.A. Kutlar, H. Arslan, and A.T. Calik, "Methods to improve efficiency of four stroke, spark ignition engines at part load," *Energy Convers. Manag.*,vol. 46, pp. 3202–3220, 2005.
[14] G. Fontana, and E. Galloni, "Experimental analysis of a spark-ignition engine using exhaust gas recycle at WOT operation," *Appl. Energy*, vol. 87, pp. 2187–2193, 2010.
[15] H.J. Parekh, B.M. Ramani, and C.J. Parekh, "Performance enhancement of internal combustion engine using weight reduction approach," *Int. J. Automot. Mech.*, vol. 15, pp. 4962-4977, 2018.
[16] B. Hu, C. Copeland, P. Lu, S. Akehurst, C. Brace, J.W.G. Turner, A. Romagnoli, and R. Martinez-Botas, "A new de-throttling concept in a twin-charged gasoline engine system," *SAE Int. J. Engines*, vol. 8, pp. 1553-61, 2015.

[17] N.D.S.A. Santos, C.E.C. Alvarez, V.R. Roso, J.G.C. Baeta, and R.M. Valle, "Lambda load control in spark ignition engines, a new application of prechamber ignition systems," *Energy Convers. Manag.*, vol. 236, pp. 114018, 2021.
[18] M.I. Jahirul, H.H. Masjuki, R. Saidur, M.A. Kalam, M.H. Jayed, M.A. and Wazed, "Comparative engine performance and emission analysis of CNG and gasoline in a retrofitted car engine," *Appl. Therm. Eng.*, vol. 30, pp. 2219-2226, 2010.
[19] S. Aljamali, W.M.F. Wan Mahmood, S. Abdullah, and Y. Ali, "Comparison of performance and emission of a gasoline engine fuelled by gasoline and CNG under various throttle positions," *J. Appl. Sci*., vol. 14, pp. 386-390, 2014.
[20] A. Kilicarslan, and M. Qatu, "Exhaust gas analysis of an eight-cylinder gasoline engine based on engine speed," *Energy Procedia*., vol. 110, pp. 459 – 464, 2017.
[21] T. Sun, Y. Chang, Z. Xie, K. Zhang, F. Chen, T. Li, and S. Yan, "Experimental research on pumping losses and combustion performance in an unthrottled spark ignition engine," *Proc. Inst. Mech. Eng. A: J. Power Energy*, vol. 232, pp. 888-897, 2018.
[22] R. Kardan, M.B. Baharom, E.M. Salah, and A.A.R. Aziz, "The effect of engine throttle position on the performance characteristics of a crank-rocker engine fitted with a conventional cylinder head," *AIP Conf. Proc.*, vol, 2035, p. 020001, 2018.
[23] R.D. Dimitrov, K.T. Bogdanov, R.Wrobel, L. Luca, MT. Karsteva, and M.M. Pasare, "Environmental characteristics of an SI engine running on methane and gasoline," presented at 7th International Conference on Energy Efficiency and Agricultural Engineering, Ruse, Bulgaria, 2020.
[24] A.A. Yontar, and Y. Doğu Y, "Investigation of the effects of gasoline and CNG fuels on a dual sequential ignition engine at low and high load conditions," *Fuel*, vol. 232, pp. 114–123, 2018.
[25] S. Postrzednik, and Z. Żmudka, "Possibility of the charge exchange work diminishing of an internal combustion engine in part load," *J. KONES*, vol. 18, pp. 377-387, 2011.
[26] M.A. Abas, W.S. Wan Salim, M.I. Ismail, S. Rajoo, and R. Martinez-Botas, "Fuel consumption evaluation of SI engine using start-stop technology," *J. Mech. Eng. Sci.*, vol. 11, pp. 2967-2978, 2017.
[27] W.S.I.W. Salim, A.A.M. Mahdi, M.I. Ismail, M.A. Abas, R. Martinez-Botas and S. Rajoo, "Benefits of spark-ignition engine fuel-saving technologies under transient part load operations," *J. Mech. Eng. Sci.*, vol. 11, pp. 3027-3037, 2017.
[28] T.I. Mohamad, and H.G. How, "Part-load performance and emissions of a spark ignition engine fueled with RON95 and RON97 gasoline: Technical viewpoint on Malaysia's fuel price debate," *Energy Convers. Manag.*, vol. 88, pp. 92835, 2014.
[29] M.F. Abdul Rahim, M.M. Rahman, and R.A. Bakar, "Cycle engine modelling of spark ignition engine processes during wide-open throttle (WOT) engine operation running by gasoline fuel," *IOP Conf. Ser. Mater. Sci. Eng.*, vol. 36, p. 012041, 2012.
[30] K.I. Hamada, M.K. Mohammed, and M.M. Rahman, "Development of a test-rig for a modern motorcycle engine," *Int. J. Automot. Mech.*, vol. 10, pp. 2034-2041, 2014.
[31] Y.F. Taha, H.J. Khalaf, and K.I. Hamada, "An assessment of the availability and efficiency of a gasoline fueled spark ignition internal combustion engine," *Energy Sources A: Recovery Util. Environ. Eff.*, 2020.
[32] K.I. Hamada, and M.M. Rahman, "An experimental study for performance and emissions of a small four-stroke SI engine for modern motorcycle," *Int. J. Automot. Mech.*, vol. 10, pp. 1852-1865, 2014.
[33] B. Sugiarto, C.S. Wibowo, A. Zikra, A. Budi, and T. Mulya, "Comparison of the gasoline fuels with octane number variations 88, 92 and 98 on the performance of 4 strokes single cylinder 150 cc spark-ignition engine," *AIP Conf. Proc.*, vol. 2062, p. 020018, 2019.
[34] E. Singh, K. Morganti, and R. Dibble, "Dual-fuel operation of gasoline and natural gas in turbocharged engine," *Fuel*, vol. 237, pp. 694-706, 2019.